

A UNITED STATES
DEPARTMENT OF
COMMERCE
PUBLICATION



NOAA Technical Memorandum NWS TDL-43

U.S. DEPARTMENT OF COMMERCE
National Oceanic and Atmospheric Administration
National Weather Service

Air-Sea Energy Exchange in Lagrangian Temperature and Dew Point Forecasts

RONALD M. REAP

Systems
Development
Office

SILVER SPRING, MD.

October 1971

M. A. ALAKA

NOAA TECHNICAL MEMORANDA

National Weather Service, Techniques Development Laboratory Series

The primary purpose of the Techniques Development Laboratory of the Office of Systems Development is to translate increases of basic knowledge in meteorology and allied disciplines into improved operating techniques and procedures. To achieve this goal, the Laboratory conducts and sponsors applied research and development aimed at the improvement of diagnostic and prognostic methods for producing weather information. The Laboratory performs studies both for the general improvement of prediction methodology used in the National Meteorological Service System and for the more effective utilization of weather forecasts by the ultimate user.

NOAA Technical Memoranda in the National Weather Service Techniques Development Laboratory series facilitate rapid distribution of material which may be preliminary in nature and which may be published formally elsewhere at a later date. Publications 1 to 5 are in the former series, Weather Bureau Technical Notes (TD), Techniques Development Laboratory (TDL) Reports; publications 6 to 36 are in the former series, ESSA Technical Memoranda, Weather Bureau Technical Memoranda (WBTM). Beginning with TDL 37, publications are now part of the series NOAA Technical Memoranda, National Weather Service (NWS).

Publications listed below are available from the National Technical Information Service, U.S. Department of Commerce, Sills Bldg., 5285 Port Royal Road, Springfield, Va. 22151. Price: \$3.00 paper copy; \$0.95 microfiche. Order by accession number shown in parentheses at end of each entry.

ESSA Technical Memorandum

- WBTM TDL 6 A Fortran Program for the Calculation of Hourly Values of Astronomical Tide and Time and Height of High and Low Water. N. A. Pore and R. A. Cummings, January 1967. (PB-174 660)
- WBTM TDL 7 Numerical Experiments Leading to the Design of Optimum Global Meteorological Networks. M. A. Alaka and F. Lewis, February 1967. (PB-174 497)
- WBTM TDL 8 An Experiment in the Use of the Balance Equation in the Tropics. M. A. Alaka, D. T. Rubsam, and G. E. Fisher, March 1967. (PB-174 501)
- WBTM TDL 9 A Survey of Studies of Aerological Network Requirements. M. A. Alaka, May 1967. (PB-174 984)
- WBTM TDL 10 Objective Determination of Sea Level Pressure from Upper Level Heights. William Klein, Frank Lewis, and John Stackpole, May 1967. (PB-179 949)
- WBTM TDL 11 Short Range, Subsynchronous Surface Weather Prediction. H. R. Glahn and D. A. Lowry, July 1967. (PB-175 772)
- WBTM TDL 12 Charts Giving Station Precipitation in the Plateau States from 700-Mb. Lows During Winter. D. L. Jorgensen, A. F. Korte, and J. A. Bunce, Jr., October 1967. (PB-176 742)
- WBTM TDL 13 Interim Report on Sea and Swell Forecasting. N. A. Pore and W. S. Richardson, December 1967. (PB-177 038)
- WBTM TDL 14 Meteorological Analysis of 1964-65 ICAO Turbulence Data. DeVer Colson, September 1968. (PB-180 268)
- WBTM TDL 15 Prediction of Temperature and Dew Point by Three-Dimensional Trajectories. Ronald M. Reap, September 1968. (PB-180 727)
- WBTM TDL 16 Objective Visibility Forecasting Techniques Based on Surface and Tower Observations. Donald M. Gales, October 1968. (PB-180 479)
- WBTM TDL 17 Second Interim Report on Sea and Swell Forecasting. N. A. Pore and Lt. W. S. Richardson, USESSA, January 1969. (PB-182 273)
- WBTM TDL 18 Conditional Probabilities of Precipitation Amounts in the Conterminous United States. Donald L. Jorgensen, William H. Klein, and Charles F. Roberts, March 1969. (PB-183 144)
- WBTM TDL 19 An Operationally Oriented Small-Scale 500-Millibar Height Analysis. Harry R. Glahn and George W. Hollenbaugh, March 1969. (PB-184 111)
- WBTM TDL 20 A Comparison of Two Methods of Reducing Truncation Error. Robert J. Bermowitz, May 1969. (PB-184 741)

(Continued inside back cover)

U. S. DEPARTMENT OF COMMERCE
National Oceanic and Atmospheric Administration
National Weather Service

NOAA Technical Memorandum NWS TDL-43

Air-Sea Energy Exchange in Lagrangian
Temperature and Dew Point Forecasts

Ronald M. Reap
Techniques Development Laboratory



Systems Development Office
Techniques Development Laboratory

SILVER SPRING, MD.
October 1971

UDC 551.509.313:551.509.323:551.465.7

551.46	Oceanography
.465.7	Energy exchange, sea-air
551.5	Meteorology
.509	Synoptic forecasting
.313	Numerical prediction models
.323	Temperature-dew point forecasts

CONTENTS

	<u>Page</u>
Abstract	1
Introduction	1
Lagrangian Prediction Model	2
Evaluation of Vertical Heat and Moisture Transport	4
Transformation Model	7
Evaluation of Results	16
Acknowledgments	22
References	22

AIR-SEA ENERGY EXCHANGE IN LAGRANGIAN
TEMPERATURE AND DEW POINT FORECASTS

Ronald M. Reap
Techniques Development Laboratory

ABSTRACT. The Techniques Development Laboratory three-dimensional trajectory model was updated in June 1971 to include the effects of air-sea interactions. Output from the model is currently transmitted via facsimile for use as guidance in severe storm forecasting. Past verification statistics for the model have shown a marked tendency to under-forecast surface temperature and dew point along coastal areas during the cold seasons. A quasi-dynamical model was developed to correct the bias in the forecasts by simulating the addition of latent and sensible heat to a column of air moving over water along a surface trajectory. Subsequent changes in the surface air temperature were assumed to be a function of the initial lapse rate, initial air temperature, sea-surface temperature, and length of over-water trajectory. Effects of the air-sea heat and moisture flux-simulation were tested for 41 cases. Verification statistics for 80 RAOB stations showed significant reductions in the root-mean-square-error and bias, resulting from the elimination of large errors in a relatively small number of forecast soundings along or near coastal waters.

INTRODUCTION

The evolution of temperature and moisture fields within the continental boundary-layer is quite often strongly influenced by the complex air-sea energy exchanges found over nearby oceans. The exchange processes occur in the form of vertical fluxes of heat, moisture, and momentum within the oceanic boundary-layer and are most pronounced whenever cold air flows over warm waters. Ideally, an accurate numerical simulation of the fluxes should entail a complete specification of the turbulent exchange coefficients. However, due to the turbulent nature of the fluxes and the small scales involved, direct measurements of the quantities needed to compute the exchange coefficients, i.e., vertical gradients of air temperature, moisture and wind speed, have been difficult, if not impossible to obtain.

For purposes of numerical simulation, the exchange coefficients and associated transport processes are usually represented by empirical formulations derived from field and laboratory experiments. Such formulations normally involve easily measured time-averaged quantities, e.g., surface wind speed, surface air temperature, and sea-surface temperature. The indirect estimates of the air-sea exchange provided by these equations, while subject to varying degrees of error, are extremely valuable in gaining physical insight into the role of the exchange processes in modifying synoptic-scale weather systems. Also, from an operational viewpoint, the empirical formulations provide a means to improve current forecasts from existing numerical models. It is the purpose of this paper to describe the simulation of air-sea interactions in the Lagrangian model (Reap 1968) developed at the Techniques Development Laboratory (TDL).

LAGRANGIAN PREDICTION MODEL

Forecasts of temperature, dew point, relative humidity, and 12-hour net vertical displacement for 24 hours in advance from the TDL trajectory model (see figure 1) are currently transmitted over the National Weather Service Forecast Office Facsimile System (FOFAX). The underlying feature of the forecast model involves the computation of three-dimensional air parcel trajectories from operational wind forecasts generated by the six-layer primitive equation model (Shuman and Hovermale 1968) currently in operation at the National Meteorological Center (NMC). A two-hour time step is employed in the iterative scheme used to compute the trajectories. Detailed forecasts of temperature and moisture are subsequently derived by computing the six-hourly variations of potential temperature and mixing ratio for air parcels assumed to follow paths defined by the trajectories. Specification of the initial temperature and moisture fields at the trajectory origin or upwind points is provided by an objective analysis technique (Endlich and Mancuso 1968) which is capable of reproducing detailed patterns and gradients with only light smoothing of the observations. Two important features of the analysis scheme involve the use of original radiosonde reports, including significant-level data, and a modified weighting function whereby observations along the flow are given greater weight than crosswind observations. This latter feature tends to preserve narrow, low-level tongues of temperature and moisture. Influences of a relatively detailed terrain are also included in the forecast program. The terrain is defined on a grid with a mesh length of approximately 120 miles, or one-half that of the NMC mesh.

Verification statistics (Reap 1968) have indicated a significant improvement over corresponding forecasts in the lowest 150 mb from the NMC six-layer model. However, a definite under-forecasting of low-level temperature and moisture was noted for the cold seasons in regions subjected to flow from nearby oceans. Errors arising under such circumstances are at least partially due to the neglect of diabatic heating of cold air flowing over warmer waters.

EVALUATION OF VERTICAL HEAT AND MOISTURE TRANSPORT

Annual or seasonal aspects of the vertical energy exchange over oceans have been investigated by many authors, including Jacobs (1951) and Budyko (1956). These and similar studies have clearly shown that solar heating and evaporation from the sea-surface represent the principal energy components in the seasonal heat balance. However, short-term computations of the air-sea energy exchange have been scarce. Some exceptions are found in the studies by Laevastu (1965), concerning the formulation of air-sea exchange processes in a manner suitable for routine analysis and prediction at the U. S. Fleet Numerical Weather Facility, and the investigation by Petterssen, Bradbury, and Pedersen (1962), describing latent and sensible heat changes in relation to Norwegian cyclone models. A similar investigation of the air-sea exchange was performed by Garstang (1967) on low-latitude synoptic-scale systems. In the preceding studies, the short-term meteorological implications and relationships between the heat exchange patterns and observed weather were discussed in considerable detail. It was found that longer-term effects resulting from the solar and terrestrial radiation balance can be neglected for short-range forecasts. This is especially true in higher latitudes where the diurnal variation of the sea-surface temperature is negligible relative to the interdiurnal changes due to moving weather systems. Therefore, latent and sensible heat transports represent the bulk of the air-sea exchange and are considered to be of primary importance in synoptic analysis and short-range prognosis.

The vertical unit-area fluxes of heat, moisture, and momentum can be described by the following standard relations:

$$Q_H = -c_p \rho K_H \left(\frac{\partial \bar{\theta}}{\partial z} \right) \quad (1)$$

$$Q_E = -\rho K_E \left(\frac{\partial \bar{q}}{\partial z} \right) \quad (2)$$

$$\tau = \rho K_M \left(\frac{\partial \bar{u}}{\partial z} \right) \quad (3)$$

where c_p is the specific heat at constant pressure, ρ is the air density, K_H , K_E , and K_M are the eddy transfer coefficients for heat, water vapor, and momentum, θ is the potential temperature, q is the specific humidity, u is the wind component along an axis parallel to the flow, and z is the height. The bar denotes an average over a period of time at a fixed point. Forming the ratio between the heat and momentum flux quantities and approximating the derivatives between the sea surface s and height z , we can write:

$$\frac{Q_H}{\tau} = c_p \frac{K_H}{K_M} \frac{\theta_s - \theta_z}{u_z} \quad (4)$$

$$\frac{Q_E}{\tau} = \frac{K_E}{K_M} \frac{q_s - q_z}{u_z} \quad (5)$$

where u_s is assumed to be zero. The vertical flux of horizontal momentum τ , or turbulent shear stress, can also be written as:

$$\tau = \rho C_z V_z^2 \quad (6)$$

where C_z is the drag coefficient appropriate to the height z , usually 10 meters, and V_z is the total wind speed. The quantity τ also represents the tangential stress exerted by the wind on the sea surface and is generally regarded as constant with height in the first few meters of the oceanic boundary-layer. Substituting for τ in (4) and (5) from (6) gives:

$$Q_H = c_p \rho C_z \frac{K_H}{K_M} (\theta_s - \theta_z) V_z \quad (7)$$

$$Q_E = \rho C_z \frac{K_E}{K_M} (q_s - q_z) V_z \quad (8)$$

where θ_s and q_s are derived from the sea-surface temperature.

In applying (7) and (8) to daily computations of the air-sea energy exchange, additional assumptions have to be made concerning the relationships between K_H , K_E , and K_M . Under stable conditions, K_H is generally less than K_M , while for strongly unstable stratification, K_H can become much larger than K_M . This finding is not surprising, especially over land, in light of the buoyancy processes which occur in highly unstable conditions, e.g., strong heating in the lower-levels due to solar radiation. In contrast, as shown by Charnock and Ellison (1959), observational evidence obtained over the sea surface leads to a somewhat different interpretation. Their measurements indicated that temperature and humidity fluctuations at 134 meters in maritime air were highly correlated, under both stable and unstable conditions. They subsequently concluded that the processes transferring heat and water vapor were identical; which implies that K_H and K_M were also equal in magnitude. Assuming the equality, $K_H = K_E = K_M$, (7) and (8) become:

$$Q_H = c_p \rho C_z (\theta_s - \theta_z) V_z \quad (9)$$

$$Q_E = \rho C_z (q_s - q_z) V_z \quad (10)$$

The derivation leading to (9) and (10) describes the well-known bulk aerodynamic method. This approach has been widely used for computations of the large-scale features of the air-sea energy exchange using climatological data derived from ship observations. According to Webb (1960), estimates for various time scales indicate that the standard error in evaluating (10) amounts to less than 10, 5, or 3.5 percent for daily, weekly, or monthly values, respectively. From a synoptic viewpoint, the bulk aerodynamic equations are entirely adequate, unless extreme instabilities exist which result in turbulent motions more intense than the neutral equilibrium case. As shown by Garstang (1967), conditions over the oceans, at least in the lower latitudes, are by and large relatively close to neutral equilibrium. The largest exchanges normally occur at times of strong winds with the associated vertical wind shear acting to maintain a near-neutral stratification by means of vigorous turbulent mixing. Consequently, as noted by Garstang (1967), the more intense the transfer, the more accurately (9) and (10) predict it. The largest errors in applying the aerodynamic equations will occur in the unlikely case where the wind is nearly calm and the air-sea temperature difference remains large. However, even in this case the exchanges are small and perhaps even negligible.

The problem now remains of evaluating the drag coefficient C_z in (9) and (10). This coefficient is found to be a function of height above the surface, atmospheric stability, and the dynamic roughness which at sea is a complex aerodynamic quantity reflecting the interaction between wind and waves. While essentially independent of the wind speed over land, the empirical formulation of C_z as a function of wind speed over the ocean has not been satisfactorily resolved (Roll 1965). If we assume that near-neutral stratification prevails, the linear variation of C_z with wind speed at 10 meters can be determined from the relation:

$$C_{10} = (1.00 + 0.07 V_{10}) \times 10^{-3} \quad (11)$$

as given by Deacon and Webb (1962), where V_{10} is in m/sec. Equation (11) expresses the corresponding dependence of the drag coefficient upon the roughness of the sea surface, as estimated from the surface wind speed. A note of caution concerning (11) is expressed since the dependence of C_z upon the wind speed is most likely nonlinear (Roll 1965). However, in the absence of more definitive information, the useful approximation for C_z given by (11) is accepted with an upper limiting value of 2.6×10^{-3} . This value agrees closely with maximum values for C_z obtained by numerous investigators, as documented by Roll (1965).

TRANSFORMATION MODEL

Having parameterized the latent and sensible heat fluxes within the first few meters of the oceanic boundary-layer, it is necessary to model the subsequent redistribution of this heat within a column of air moving over the ocean. Following Burke (1945), Davis et al., (1968), and others, a quasi-dynamical model is developed in which the form of the forecast, or transformed sounding, is assumed. In essence, we are assuming that the modified air lies completely under unmodified air, i.e., we do not apply the diffusion equation. This assumption constitutes the principal empirical component of the model. However, it must be noted that the assumed form of the forecast sounding agrees quite well with features observed over water under lapse conditions (Klein 1946). The modified sounding, as shown in figure 2, is characterized by the following regions:

1. A contact layer extending from the sea-surface to approximately 10 meters. This layer exhibits a strongly superadiabatic lapse rate, a marked upward decrease in the mixing ratio, and constant fluxes of latent and sensible heat associated with the pronounced vertical gradients of temperature and moisture.
2. A well-mixed layer extending from the top of the contact layer to the lifting condensation level (LCL). This layer normally exhibits nearly constant values of potential temperature and mixing ratio.
3. A saturated region or cloud layer above the mixed layer extending to the height, usually associated with the cloud tops, at which the saturated adiabat through the LCL intersects the initial sounding.

Although the assumed form of the forecast sounding agrees in general with features observed over water under lapse conditions, the transport processes effecting the actual transformation may be quite complex. For example, within the saturated layer, convective cells in the form of cumulus clouds play a dominant role in the vertical transport of energy. Within the mixed layer, conditions favor strong vertical transport by means of turbulent eddies. These same conditions, i.e., pronounced vertical wind shear, large air-sea temperature difference, and near-neutral stability, also favor the generation of well-organized secondary circulations within the boundary-layer. For example, Hanna (1969) has documented the presence of longitudinal roll vortices and accompanying cloud streets whose scale is considerably larger than the individual turbulent elements. The quantitative effects of such circulations on the boundary-layer temperature and moisture profiles are only partially understood at the present time, although we may qualitatively attach some importance to them. However, it would be inappropriate to attempt refinements of this type in the present model, since any variations in the vertical profiles due to secondary boundary-layer circulations are probably much smaller than the errors inherent in the wind forecasts used to compute the trajectories.

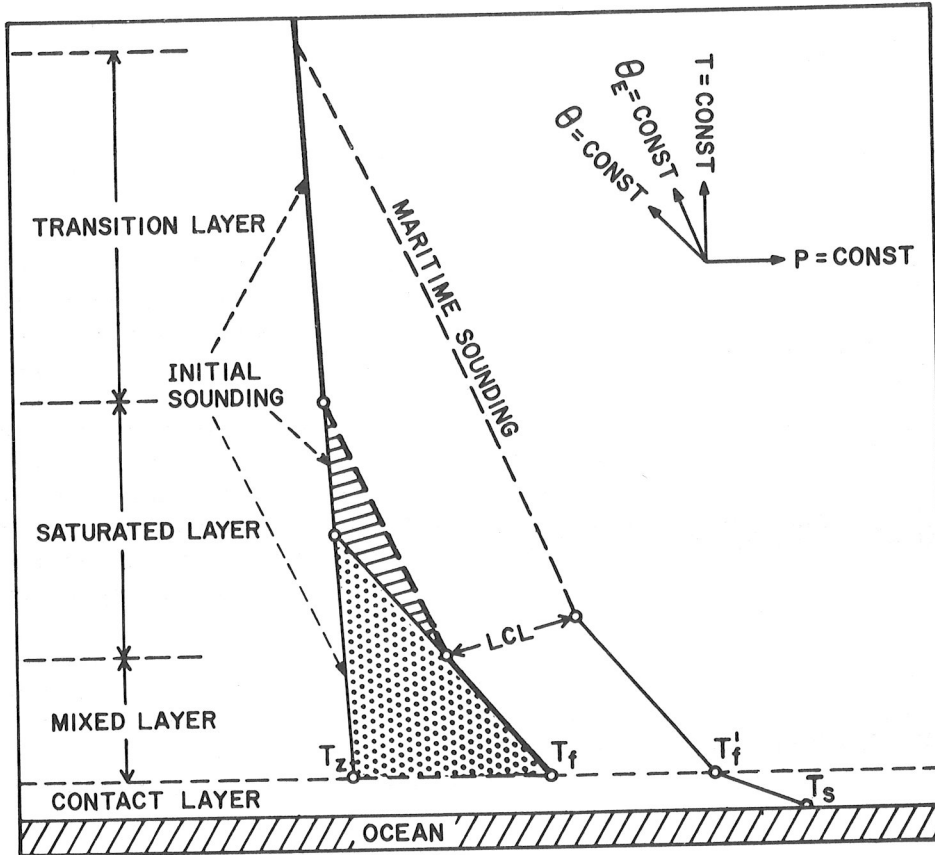


Figure 2. Heavy curve portrays modified sounding with dashed lines denoting saturated ascent. The predicted increase in surface air temperature from an initial value T_z to the final value T_f corresponds to an intermediate phase of the transformation process. For a sufficiently long over-water path, T_f will approach T_f' , which is the equilibrium air temperature with respect to the sea-surface temperature T_s .

a) Temperature

We will now develop the model equations for determining the final surface air temperature (T_f). Following Burke (1945), T_f is defined by the functional relationship:

$$T_f = \Psi (T_z, S, B, T_s)$$

where T_z is the initial surface air temperature ($^{\circ}\text{A}$), S is the length (km) of the overwater trajectory, B is the initial lapse rate ($\Delta T / \Delta \ln p$), and T_s is the mean sea-surface temperature ($^{\circ}\text{A}$). More concisely, we wish to obtain Ψ in the form of an analytical solution for the surface air temperature at any

phase of the transformation process. As previously noted, the long-term effects of the radiation balance are neglected. We can now express the individual change in the heat content of a moving column of unit cross-section by:

$$\frac{d}{dt} (\Delta H) = \frac{\partial}{\partial t} (\Delta H) + V_z \frac{\partial}{\partial s} (\Delta H) \quad (12)$$

where s is distance along the trajectory, V_z is the mean wind speed along s , and ΔH is the difference between the instantaneous and original heat content of the column. Assuming steady-state, i.e., local effects due to radiation, condensation, etc. are neglected, we can write:

$$\frac{d}{dt} (\Delta H) = Q_H = V_z \frac{\partial}{\partial s} (\Delta H) \quad (13)$$

and from (9), noting that $T \approx \theta$ at sea level, we have

$$c_p \rho C_z (T_s - T_z) V_z = V_z \frac{\partial}{\partial s} (\Delta H) \quad (14)$$

To evaluate the right-hand side of (14), let us express the heat content H of the column up to the upper limit of temperature convection as:

$$H = \frac{c_p}{g} \int_p^{p_0} T(s,p) dp \quad (15)$$

where p_0 is the surface pressure and p is the pressure at the top of the mixed layer. At $s = 0$

$$H_0 = \frac{c_p}{g} \int_p^{p_0} T(0,p) dp \quad (16)$$

We can now write (14) as:

$$c_p \rho C_z (T_s - T_z) V_z = \frac{V_z c_p}{g} \frac{\partial}{\partial s} \int_p^{p_0} [T(s,p) - T(0,p)] dp \quad (17)$$

At this point we deviate from Burke's derivation and introduce the initial and final temperature profiles in the form suggested by Duquet (1960), namely:

$$T(o,p) = T(o,p_o) + B \ln(p/p_o) \quad (18)$$

$$T(s,p) = T(s,p_o) + \beta \ln(p/p_o) \quad (19)$$

where β is the value of B when the lapse rate is dry-adiabatic. If we introduce the temperature profiles in this manner into (17), the resulting integral can be evaluated analytically to give:

$$X - Y \ln \left(\frac{Y}{Y-X} \right) = \frac{gC_{10}}{R} \frac{S}{T_s} (B - \beta) \quad (20)$$

where $X = T_f - T_z$, $Y = T_s - T_z$, g is gravity, $C_z = C_{10}$ is given by (11), and R is the gas constant for dry air. In essence, (20) represents the position of the final dry-adiabat (figure 2) as obtained from the time integrals over the sensible heat flux (9). Solutions for T_f can be quickly obtained by iteration procedures on an electronic computer. This is in contrast to the rather complicated plates and graphs originally designed by Burke (1945) to aid the operational forecaster in estimating the degree of air-mass modification for cold air flowing over warmer waters.

The sea-surface temperatures needed to compute T_s in (20) are extracted from analyzed fields transmitted to NMC from the U.S. Fleet Numerical Weather Facility (FNWF). The analyses are frequently updated at FNWF to include all available ship reports. A typical analysis for United States coastal waters is shown in figure 3.

According to Burke (1945) and Klein (1946), the final sea temperature is more important than the mean sea temperature in determining the final air temperature T_f . This was confirmed in the present study by comparing forecasts run for several cases using both mean sea temperatures and final sea temperatures. Therefore, for over-water distances (S) greater than 650 km, T_s is set equal to the final sea temperature T_{sf} . For S less than 650 km, T_s is set equal to $(T_{si} + 3T_{sf})/4$, where T_{si} is the initial sea temperature.

Additional quantities needed to determine T_s , C_{10} , S , and B in (20) are derived from the basic six-hour surface forecasts of parcel position and temperature produced by the TDL trajectory model. Briefly, the derived quantities consist of the following:

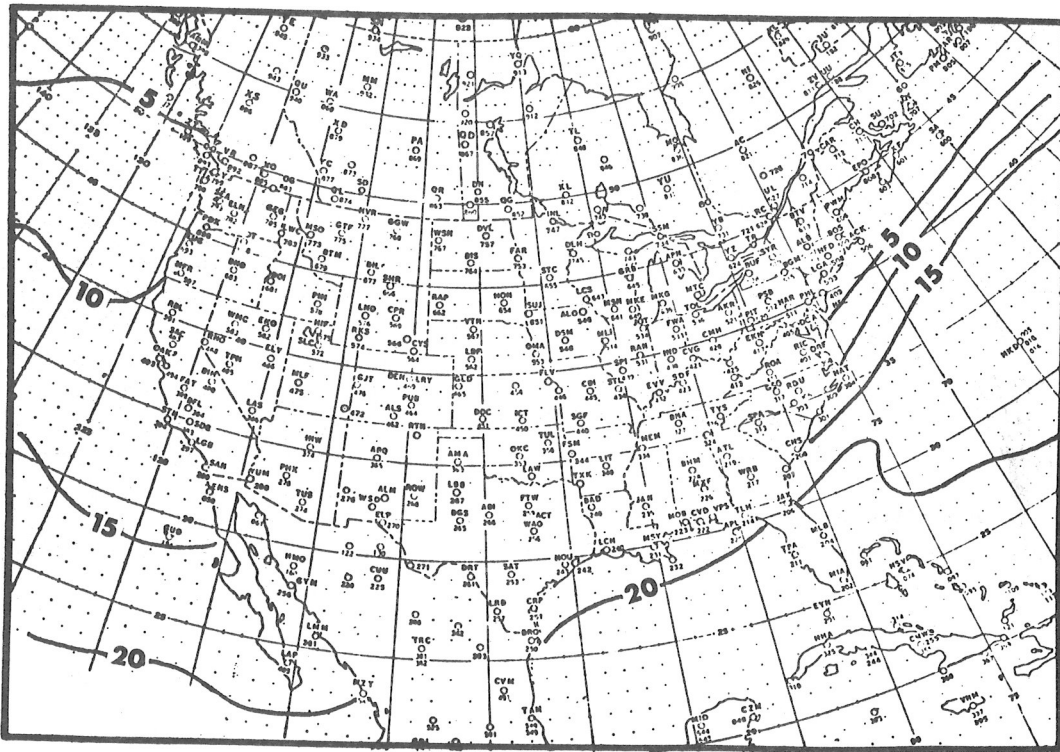


Figure 3. FNWF sea-surface temperature ($^{\circ}\text{C}$) analysis for 0000 GMT on March 23, 1969.

- (a) Parcel temperature and x,y,p,t coordinates at landfall,
- (b) Total over-water time (hr),
- (c) Total distance (km) of over-water path, including single or multiple over-water segments,
- (d) Average sea-surface temperature for each six-hour segment of the trajectory during which the parcel was over-water.

Inspection of (20) reveals that most of the parameters on the right-hand side can be calculated in a rather direct and reasonably accurate manner. However, determination of the initial lapse rate B presents special problems. To obtain this quantity it is necessary to know when and where the surface trajectories cross the coastline. This is accomplished by computing the x,y,p,t, landfall coordinates from the basic six-hour trajectory forecasts of parcel position. The initial lapse rate for the vertical column is then computed from the temperatures extracted for various levels at the point where the surface trajectory crosses the coastline. We further assume that the column of air moves along the surface trajectory. The last assumption is strictly satisfied only when the trajectories show little variation with height. However, substantial variations of trajectory with height are found in most operational forecasts. In addition, the lapse rate within the column also

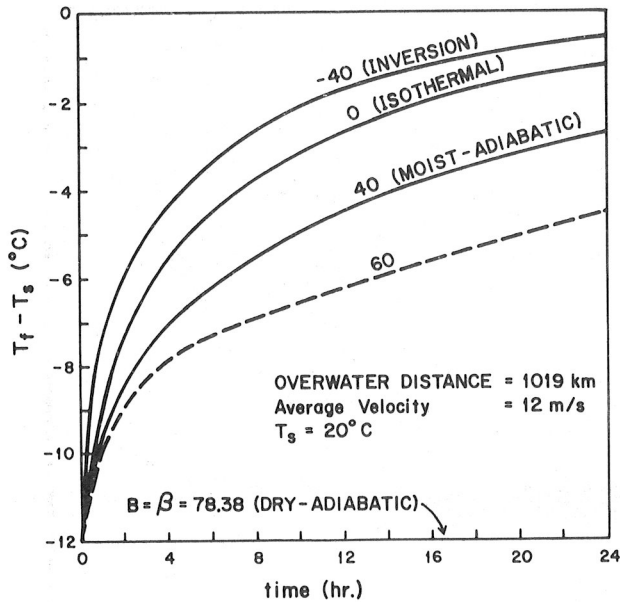


Figure 4. Modification of surface air temperature T_f as a function of initial lapse rate B , sea-surface temperature T_s , and time, for a typical 24-hr forecast. $B = \Delta T / \Delta(\ln p)$, where T is temperature and p is pressure. For B dry-adiabatic, no change occurs in T_f , i.e., the forecast curve lies along the abscissa.

varies during the forecast period in response to synoptic-scale vertical motions. Therefore, it would appear desirable to combine the initial and unmodified final sounding in some appropriate manner to give an "average" lapse rate B for the transformation process. However, if we refer to figure 4, which gives a typical family of solution curves for T_f as a function of time over water and varying initial lapse rate B , it appears that most of the temperature change occurs within the first six to eight hours. Hence, for a wide range of atmospheric stability, the initial lapse rate is of primary importance in determining the change in the surface air temperature. This is especially true for short over-water travel times, in which case the trajectory variations with height and the changes due to synoptic-scale vertical motions are usually slight.

Referring again to figure 4, we note a very slow increase in the surface air temperature for initial lapse rates approaching the dry-adiabatic value. In the limiting case, (20) reduces to:

$$\lim_{B \rightarrow \beta} \Psi(T_z, S, B, T_s) = 0 \quad (21)$$

That is, a slight increase in the initial surface air temperature T_z corresponds to heating a column of infinite vertical extent since the final dry-adiabat through T_f parallels and does not intersect the initial sounding, which is also dry-adiabatic. It is clear that (20) breaks down when B

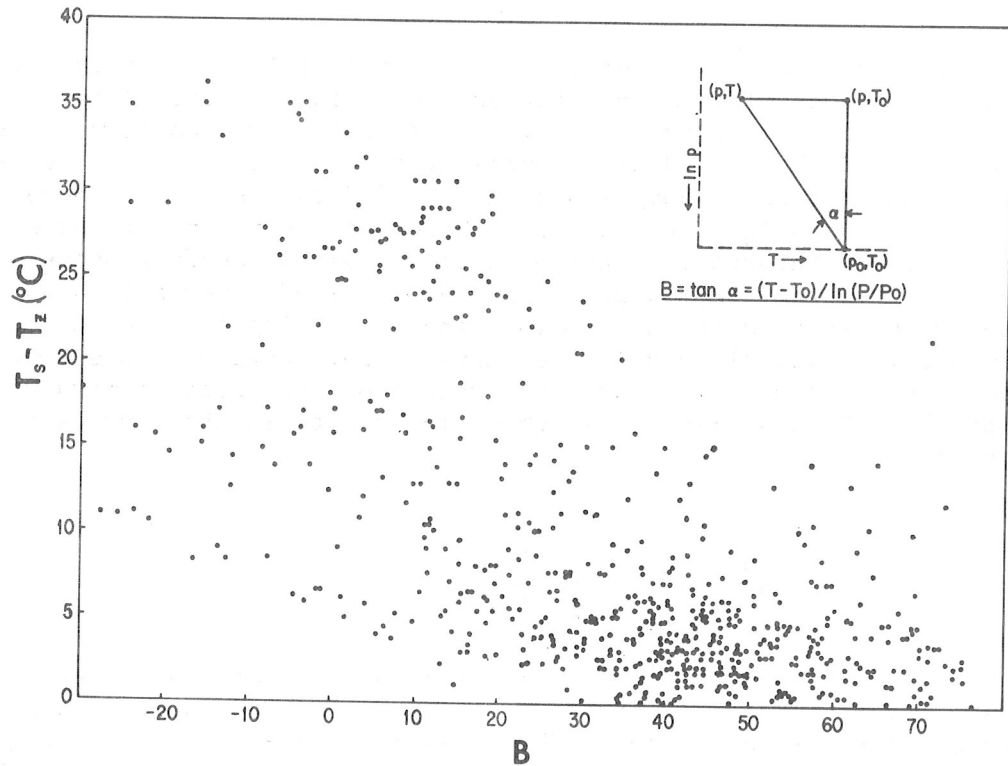


Figure 5. Plot of the initial lapse rate B (surface-850mb) versus the initial air-sea temperature difference ($T_s - T_z$) for 600 over-water trajectories.

approaches or equals β , since little or no temperature rise is forecast. Hence, (20) fails to simulate the often significant addition of sensible heat to initially well-mixed cold polar air passing over warmer waters. However, such well-mixed layers are normally shallow with stable lapse rates aloft inhibiting the vertical heat transport. Referring to figure 5, we find that only 10 percent of the cases from a representative sample have initial lapse rates greater than 60 for the surface to 850-mb layer. The dry-adiabatic value ranges between 68-83, increasing with temperature. Only 2 percent of the cases have an initial air-sea temperature difference greater than 5°C with an initial lapse rate of 60 or higher. Thus, the problem of calculating the addition of heat to an initially well-mixed layer is circumvented by selecting the top of the layer, for which B is defined, high enough so that a reasonable value of B can be computed. Normally, the 850-mb level was found to be satisfactory in this respect. However, when the surface to 850-mb layer is dry-adiabatic, mid-level (700 mb) temperatures are also used in determining the initial lapse rate.

During the operational procedure, an attempt is made to determine B as accurately as possible. As a first approximation, a preliminary forecast of T_f is made from (20) using an initial lapse rate computed from the surface (T_z) and 850-mb (T_{85}) landfall temperatures. If the initial lapse rate is dry-adiabatic, it is re-computed using the 700-mb landfall temperature in addition to T_z and T_{85} . A check is subsequently performed to determine if the dry-adiabat through T_f intersects the original sounding above 850 mb. If this occurs, the temperature T_c at the level of intersection is computed and subsequently used in conjunction with T_z and T_{85} to calculate a more representative initial sounding and lapse rate. However, some smoothing is required to obtain a linear lapse rate from the three temperatures T_z , T_{85} , and T_c . A mean pressure-weighted lapse rate is obtained using the expression:

$$\frac{\overline{\Delta T}}{\Delta P} = \sum_{k=1}^n \Delta T_k \Delta P_k / \sum_{k=1}^n \Delta P_k^2 \quad (22)$$

where ΔT_k and ΔP_k are the temperature and corresponding pressure increments for each layer. The forecast for T_f is then repeated using this new or "adjusted" lapse rate in (20). The preliminary forecast is accepted only in the case where the dry-adiabat through T_f intersects the original sounding below 850 mb. In this case, the solution of (20) indicates that the top of the mixed layer has not penetrated above the 850-mb level, i.e., the initial lapse rate B is representative of the layer undergoing modification.

b) Moisture

Having estimated the final surface air temperature T_f for a column of air moving along the surface trajectory, we will now examine the problem of forecasting moisture changes within the mixed layer. It is possible to use (10) to compute the moisture flux at the top of the contact layer; however, the subsequent redistribution of this moisture through the subcloud layer is considerably more complex than in the case of temperature, where the final lapse rate given by (19) is assumed to be dry-adiabatic. Normally, a constant value of specific humidity is associated with a well-mixed subcloud layer in equilibrium with the sea-surface. However, numerous analyses of ship soundings, see e.g., Klein (1946), have revealed a definite decrease of specific humidity with height in the dry-adiabatic layer during the transformation from continental to maritime air. It appears that the observed gradients of specific humidity are closely related to the intensity of the vertical turbulent transport. Hence, a wide variety of moisture profiles is possible within the subcloud layer. Consider, for example, the case where the upward turbulent transport at the top of the subcloud layer is greater than the evaporation from the ocean surface. In the absence of horizontal moisture convergence, the surface layer will subsequently lose moisture and dry out. As noted by Riehl and Pearce (1968), this process is physically

reflected in trade wind regions by the mixing of very dry air downward from an upper inversion. Under strong anticyclonic flow, it may even be possible for the surface dew points to decrease slowly or remain constant in the presence of continuing evaporation from the ocean surface.

Another mechanism for lowering the surface dew points is the intrusion of downdrafts from precipitation cooling into the surface layer. This process is most pronounced in low-level convergence zones. Significant changes in the low-level moisture content may in some instances depend more upon the divergence of the moisture flux than evaporation from the ocean surface. Additional evidence supporting this viewpoint was provided by Riehl and Pearce (1968) in approximating the total heat change following a surface trajectory in the tropics by:

$$\frac{dH}{dt} = L V_z \frac{\partial q}{\partial s} \quad (23)$$

where L is the latent heat of evaporation and q is the specific humidity. The sensible heat flow was neglected in (23) since the heat energy represented by the latent heat flux is approximately 5 to 10 times greater, except in disturbances where the sensible heat flow may be proportionately enhanced (Garstang 1967). Little correlation was found between the centers of evaporation, as determined from an equivalent form of (10), and dH/dt computed from (23). That is, there is no simple relationship between the latent heat flux and the moisture content of the subcloud layer.

As a consequence of the difficulties in predicting moisture changes in the subcloud layer, an "average" relative humidity of 65 percent, obtained from studies by Klein (1946), is assumed at the ocean surface, except in cases where the initial dew point results in values greater than 65 percent. The final surface dew points are subsequently derived from the forecast air temperature (T_f) and the assumed surface relative humidity.

The final step in the transformation process is accomplished by adjusting the 850-mb temperature and dew point forecast. This adjustment is only carried out when the 850-mb level lies within the modified regions shown in figure 2, i.e., within the mixed or saturated layers. As a first step in the adjustment procedure, the lifting condensation level (LCL) is computed from T_f and the forecast surface dew point. If the LCL is above 850 mb, the variable T_m is set equal to the temperature at the intersection of the 850-mb level with the dry-adiabat through T_f . If the LCL is below 850 mb, T_m is set equal to the temperature at the intersection of the 850-mb level with the saturation adiabat through the LCL. Therefore, if T_m is less than the forecast 850-mb temperature, i.e., if the top of the mixed or saturated layer is below 850 mb, then no change is made to the original forecast. If T_m is greater, the forecast temperature at 850 mb is replaced by T_m .

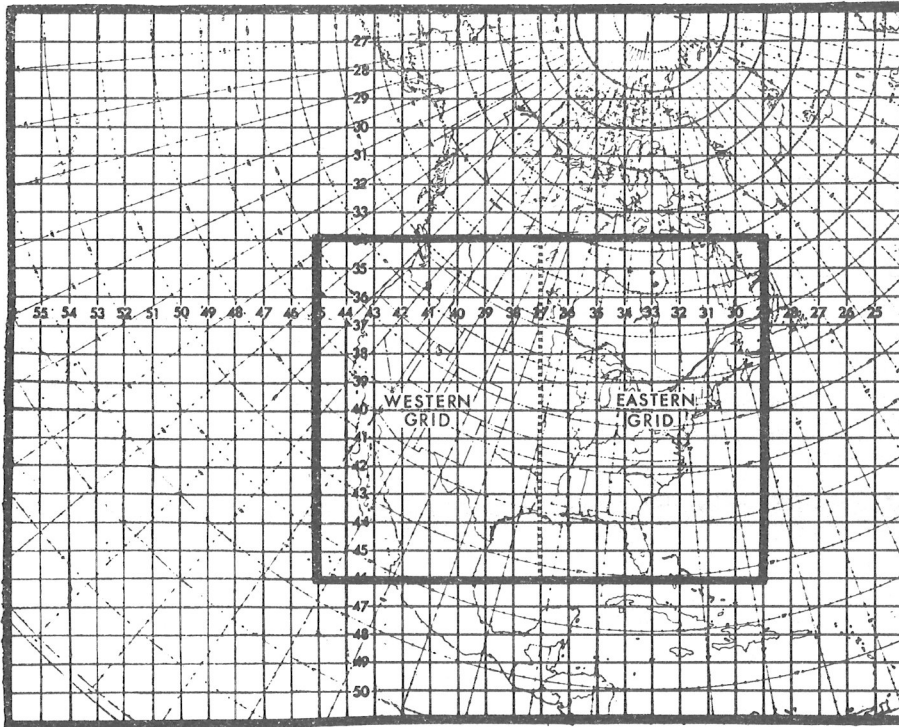


Figure 6. Temperature and dew point forecasts are verified for the 13 by 17 grid centered over the United States. The grid interval is 381 km at 60°N. Separate verifications are made for the Eastern and Western grids.

Finally, an adjusted dew point at 850 mb is computed by assuming a fixed value for the relative humidity within the saturated layer. The moisture transported aloft by convective cells in this layer during the transformation process is usually not sufficient to effect complete saturation, i.e., there is substantial entrainment and mixing with the environmental air. Hence, a reduced relative humidity of 85 percent is used to compute the adjusted 850-mb dew point. This value was obtained by experimentation and agrees with average values given by Malkus (1958) for the boundary between mixed and saturated layers.

EVALUATION OF RESULTS

The basic verification sample used in this study consisted of 41 cases run within the period January 1 to April 20, 1971. A statistical program used routinely to verify operational forecasts from the trajectory model was run to evaluate the 24-hr temperature and dew point forecasts at the surface and 850 mb for the 41-case sample. Forecast soundings at individual upper-air stations were constructed by the program from the gridded trajectory forecasts by means of bilinear interpolation. The interpolated soundings were then verified against the actual RAOB reports for all stations located within the 13 by 17 grid shown in figure 6. Each half of the grid was treated separately in order

to distinguish between forecasts for mountainous areas and those for regions having relatively flat terrain. Approximately 75 to 80 RAOB stations were verified for an average case.

Shown in table 1 are the overall error field statistics for the modified and unmodified forecasts. Noting that the number of soundings actually modified for an average case usually represents about 35 percent of the total number of soundings forecast by the trajectory model, and also that most of the modified soundings lie over the ocean where verification stations are sparse, the results from the verification program are summarized as follows:

a) The most significant improvement was achieved in the surface dew point forecasts for coastal regions east of the continental divide. The overall root-mean-square-error (RMSE) was reduced by 0.6°C and the pronounced cold season dry bias in the unmodified forecasts, as shown by the algebraic error in figure 7, was considerably reduced in both eastern and western regions.

b) The RMSE for the surface temperature forecasts was improved and the cold bias shown by the algebraic error in figure 8 was completely removed in the east and reduced in the west.

c) No appreciable differences were found in the RMSE for the 850-mb temperature forecasts. The RMSE for the 850-mb dew point forecasts showed a slight improvement in the east along with a corresponding reduction in the dry bias. However, the RMSE for 850-mb dew point forecasts in the west showed a slight rise along with a positive bias in the forecasts.

Effects of the air-sea heat and moisture-flux simulation may be examined in greater detail by referring to figures 9-10, which illustrate one of the more dramatic improvements obtained for an individual case. It is clear from figure 10 that the modified forecasts eliminate most of the error arising from neglect of air-sea interactions in the current operational trajectory model. Note also that the forecast errors are reduced some distance inland due to adjustments in the coastal temperature gradients, i.e., the predicted warming at over-water grid points is spread inland by the verification program when interpolating forecast soundings at upper-air stations located near the coastline. The remaining area of underforecast temperatures resulted from neglecting the warming of cold polar air moving overland to the Gulf Coast area. The surface trajectories plotted in figure 10 serve to illustrate this point. Further modifications planned for the trajectory model will also include attempts to correct for overland air-mass modification.

As previously noted, the improvements achieved in the RMSE resulted from the reduction of large errors in a relatively small number of forecast soundings along or near coastal waters. For example, modification of an individual forecast sounding at a grid point located near Jacksonville, Florida is shown in figure 11. Here we find the modified and unmodified

TABLE 1

Effects of air-sea heat and moisture flux in TDL 3D Trajectory Model. Statistics are based on 41 cases within the period January 14, 1971, to April 20, 1971. Verification of unmodified operational model is indicated by ().

	Linear Correlation		Root Mean Square Error (°C)		Algebraic Error (°C)	
	Temperature	Dew Point	Temperature	Dew Point	Temperature	Dew Point
Surface	.928 (.923)	.898 (.888)	4.31 (4.50)	4.62 (5.22)	0.0 (-1.0)	-0.8 (-2.4)
850 MB	.949 (.951)	.783 (.792)	2.91 (2.90)	6.51 (6.58)	0.1 (0.2)	-0.9 (-2.1)
.....						
Surface	.873 (.863)	.786 (.776)	4.65 (5.00)	5.79 (5.85)	-0.7 (-1.5)	0.2 (-0.7)
850 MB	.893 (.892)	.601 (.607)	4.13 (4.16)	6.26 (6.18)	1.2 (1.3)	0.5 (0.0)
.....						

EASTERN
U.S.

WESTERN
U.S.

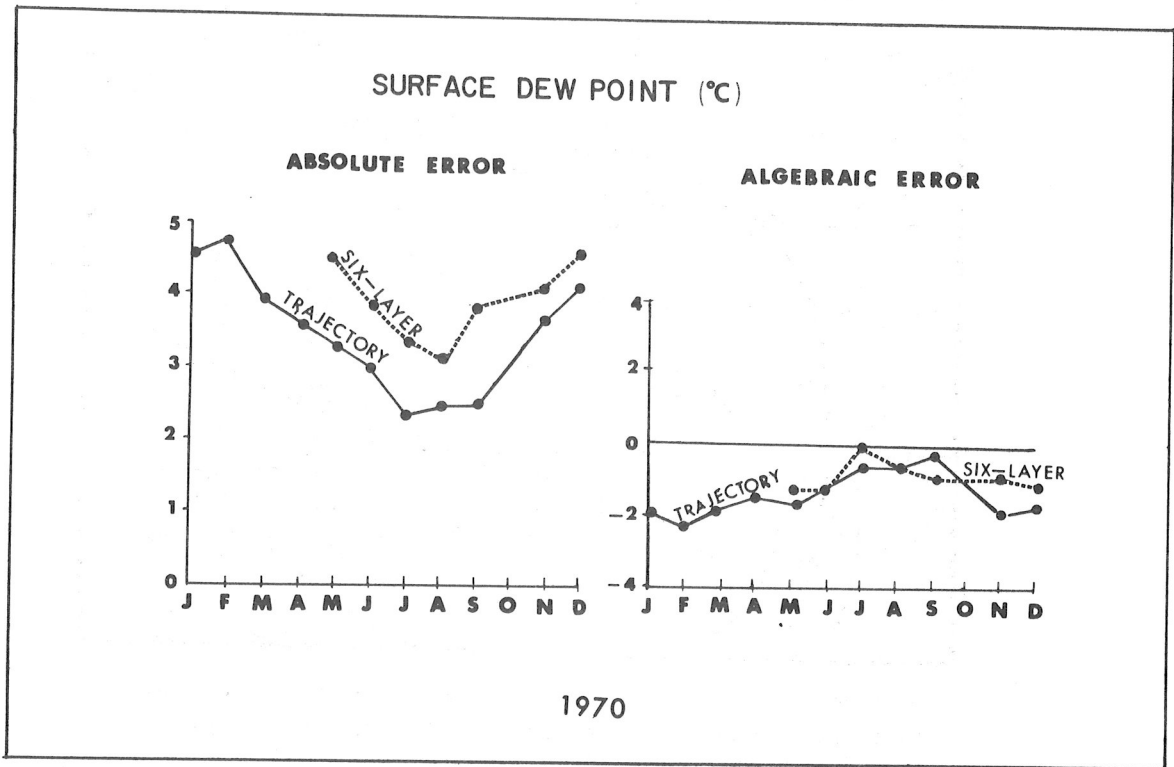


Figure 7. Verification of 24-hour surface dew point forecasts.

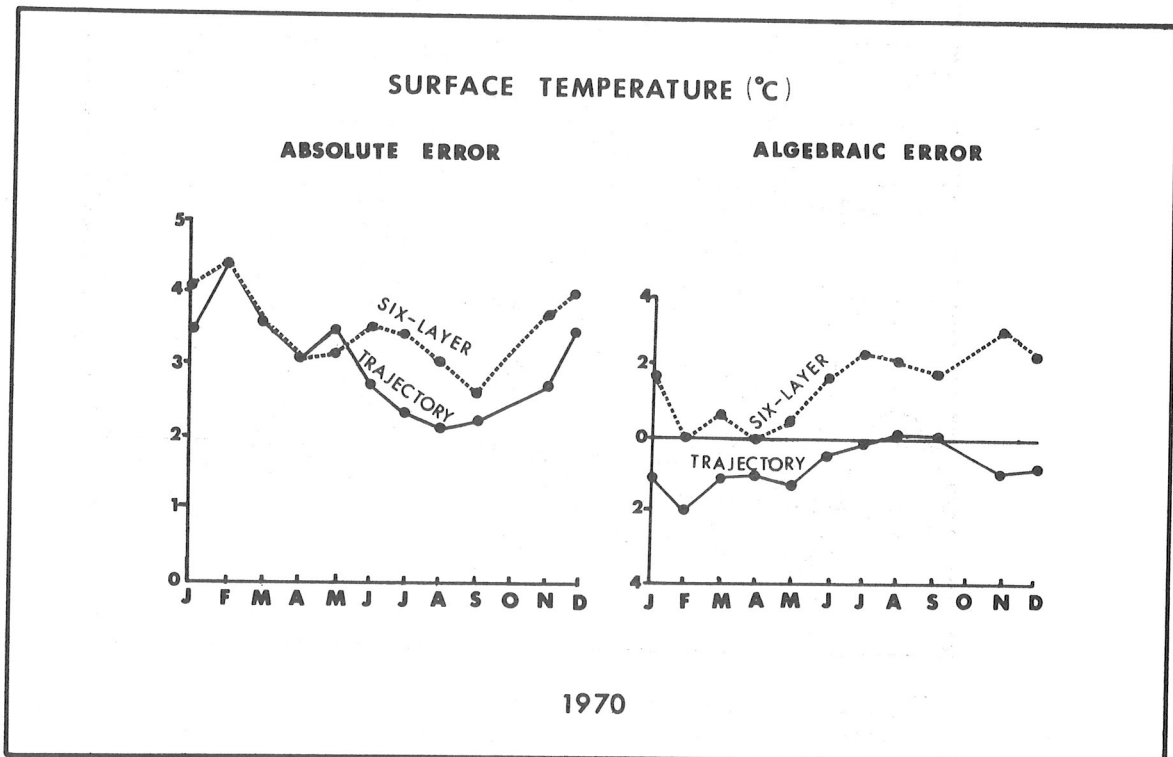


Figure 8. Verification of 24-hour surface temperature forecasts.

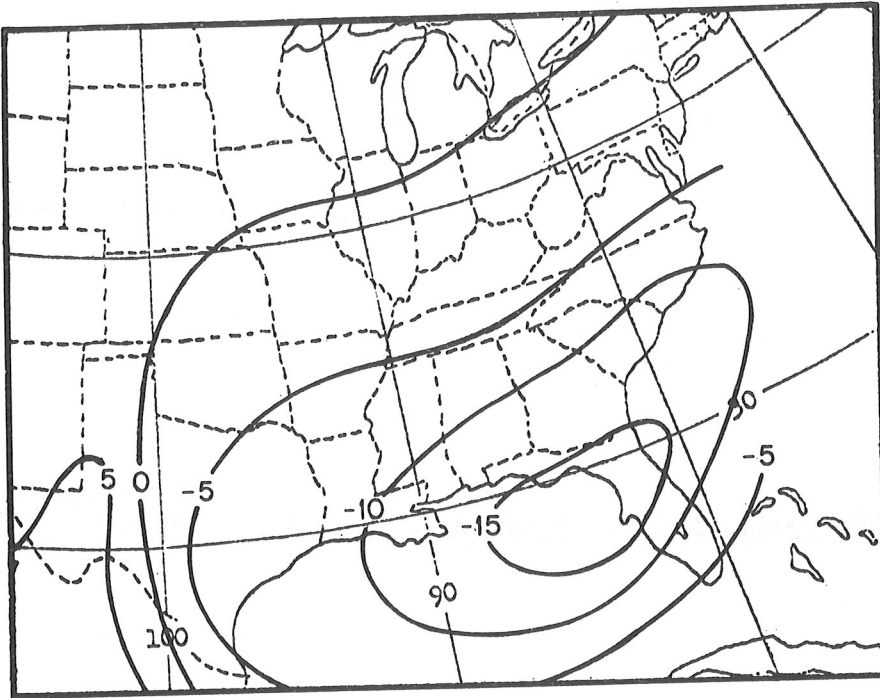


Figure 9. Surface temperature error ($^{\circ}\text{C}$) from unmodified trajectory model for 24-hour forecast verifying at 0000 GMT on February 2, 1971.

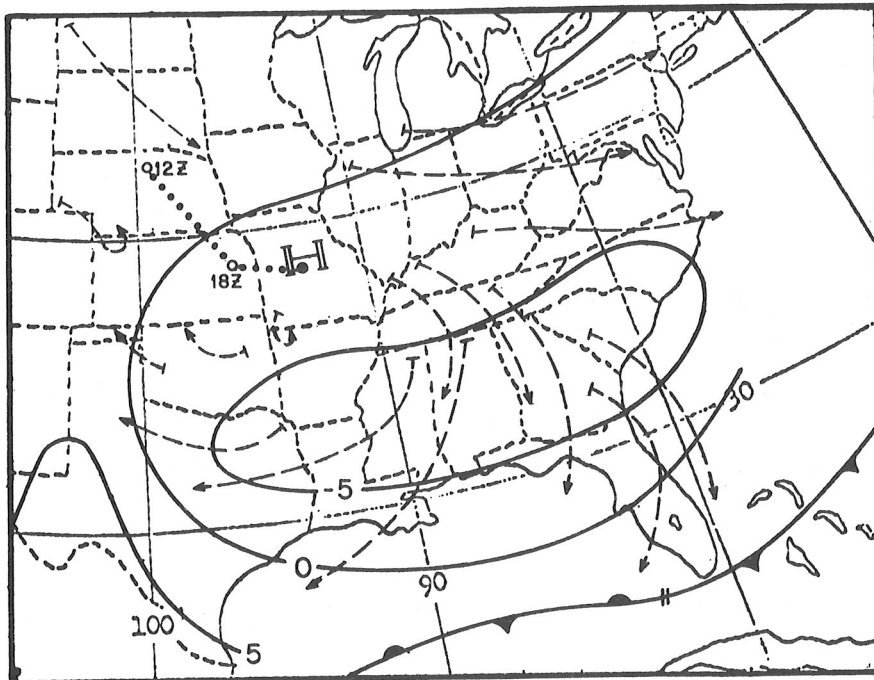


Figure 10. Surface temperature error ($^{\circ}\text{C}$) from trajectory model with air-sea heat flux simulation. Forecast verifies at 0000 GMT on February 2, 1971. Surface trajectories and movement of surface high are given by dashed and dotted lines, respectively.

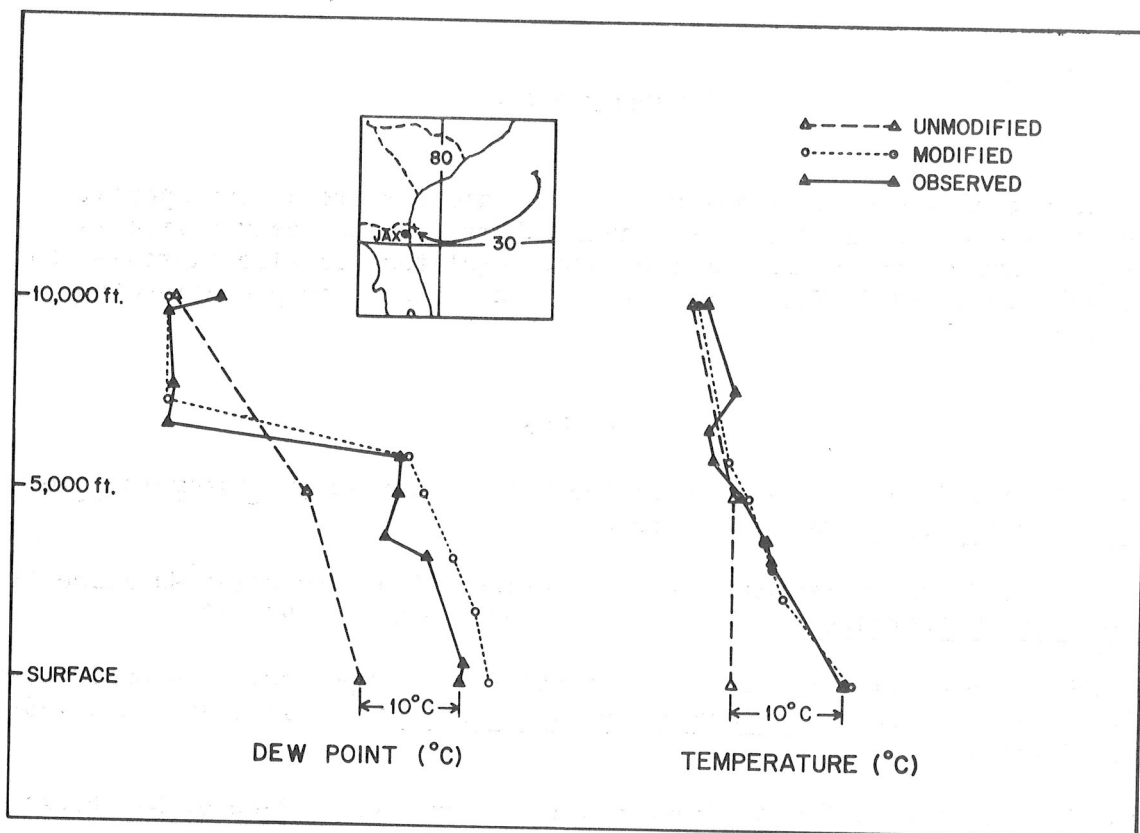


Figure 11. Modification of a forecast sounding by simulation of air-sea heat and moisture exchange. Insert shows 24-hr path of surface trajectory across the Gulf Stream terminating at a grid point located near Jacksonville (JAX), Florida. Observations at JAX were taken at 0000 GMT on March 24, 1969.

forecasts of temperature and moisture plotted against the observed profiles at Jacksonville. The path of the surface trajectory over the warm Gulf Stream is also shown in figure 11. Note that the modified sounding is specified in much greater accuracy and detail than the unmodified sounding. The additional points outlining the modified sounding lie at the lifting condensation level (LCL) and along the moist adiabat through the LCL, as previously discussed and shown in figure 2.

The operational trajectory model was updated on June 7, 1971 to include the air-sea heat and moisture-flux program. In addition, a supplementary investigation has indicated that the effects of the flux program in the trajectory model would be enhanced by allowing for compensating diabatic processes, e.g., cooling over snow or ice cover, cooling due to precipitation, etc. The introduction of a diurnal temperature wave which is sensitive to cloud cover, in itself a desirable modification, would also complement the results obtained from the flux program. The largest single source of error in the flux program lies in the low-level wind forecasts from the NMC six-layer primitive equation model; hence, any improvement in the basic wind forecasts would tend to increase the accuracy of the surface trajectories and resulting modifications by the flux program.

ACKNOWLEDGMENTS

The author wishes to thank M. A. Alaka and members of the Special Projects Branch, Techniques Development Laboratory for their advice and assistance during the course of the work. Gratitude is also expressed to D. J. Sakelarlis and B. Eastridge for their assistance in preparing the manuscript.

REFERENCES

- Budyko, M. I., "The Heat Balance of the Earth's Surface," Gidrometeorologicheskoe Izdatel'stvo, 1956, 255 pp.
- Burke, C.J., "Transformation of Polar Continental Air to Polar Maritime Air," Journal of Meteorology, Vol. 2, No. 2, June 1945, pp. 94-112.
- Charnock, H. and Ellison, T.H., "Fluctuations of Temperature and Humidity at 134 m over the Sea," Deutsche Hydrographische Zeitschrift, Vol. 12, 1959, pp. 171-180.
- Davis, L. G., et al., "Lake Effect Studies," Contract E22-80-67(N), Final Report, Pennsylvania State University, 1968, 108 pp.
- Deacon, E. L. and Webb, E. K., Interchange of Properties between the Sea and Air. "The Sea: Ideas and Observations," M. N. Hill, Editor, Vol. 1, Wiley (Interscience), New York, 1962, pp. 43-87.
- Duquet, R. T., "An Analytic Expression for the Modification of Cold Air by a Warm Surface," Journal of Meteorology, Vol. 17, No. 3, June 1960, p. 377.
- Endlich, R. M. and Mancuso, R. L., "Objective Analysis of Environmental Conditions Associated with Severe Thunderstorms and Tornadoes," Monthly Weather Review, Vol. 96, No. 6, June 1968, pp. 342-350.
- Garstang, M., "Sensible and Latent Heat Exchange in Low Latitude Synoptic Scale Systems," Tellus, Vol. 19, No. 3, 1967, pp. 492-508.
- Hanna, S. R., "The Formation of Longitudinal Sand Dunes by Large Helical Eddies in the Atmosphere," Journal of Applied Meteorology, Vol. 8, No. 6, Dec. 1969, pp. 874-883.
- Jacobs, W. C., "Large-Scale Aspects of Energy Transformation Over the Oceans," Compendium of Meteorology, American Meteorological Society, 1951, pp. 1057-1070.
- Klein, W. H., "Modification of Polar Air over Water," Journal of Meteorology, Vol. 3, No. 3, Sept. 1946, pp. 100-101.

- Laevastu, T., "Synoptic-Scale Heat Exchange and its Relations to Weather," Technical Note No. 7, Fleet Numerical Weather Facility, 1965, 28 pp.
- Malkus, J. S., "On the Structure of the Trade Wind Moist Layer," Massachusetts Institute of Technology and Woods Hole Oceanographic Institution, Papers in Physical Oceanography and Meteorology, Volume XIII, No. 2, August 1958, Cambridge and Woods Hole, Mass. 47 pp.
- Petterssen, S., Bradbury, D. L. and Pedersen, K., "The Norwegian Cyclone Models in Relation to Heat and Cold Sources," Geofysiske Publikasjoner, Vol. XXIV, No. 9, 1962, pp. 249-280.
- Reap, R. M., "Prediction of Temperature and Dew Point by Three-Dimensional Trajectories," ESSA Technical Memorandum WBTM TDL-15, 1968, 20 pp.
- Riehl, H. and Pearce, R. P., "Studies on Interaction Between Synoptic and Mesoscale Weather Elements in the Tropics," Atmospheric Science Paper No. 126, Colorado State University, Ft. Collins, Colo., 1968, 64 pp.
- Roll, H. U., Physics of the Marine Atmosphere, International Geophysics Series, Vol. 7, Academic Press, New York, N. Y., 1965, 426 pp.
- Shuman, F. G. and Hovermale, J. B., "An Operational Six-Layer Primitive Equation Model," Journal of Applied Meteorology, Vol. 7, No. 4, Aug. 1968, pp. 525-547.
- Webb, E. K., "An Investigation of the Evaporation from Lake Eucumbene," Division of Meteorological Physics Technical Paper No. 10, Australia, Commonwealth Scientific and Industrial Research Organization, Melbourne, Australia, 1960, 77 pp.

(Continued from inside front cover)

- WBTM TDL 21 Automatic Decoding of Hourly Weather Reports. George W. Hollenbaugh, Harry R. Glahn, and Dale A. Lowry, July 1969. (PB-185 806)
- WBTM TDL 22 An Operationally Oriented Objective Analysis Program. Harry R. Glahn, George W. Hollenbaugh, and Dale A. Lowry, July 1969. (PB-186 129)
- WBTM TDL 23 An Operational Subsynoptic Advection Model. Harry R. Glahn, Dale A. Lowry, and George W. Hollenbaugh, July 1969. (PB-186 389)
- WBTM TDL 24 A Lake Erie Storm Surge Forecasting Technique. William S. Richardson and N. Arthur Pore, August 1969. (PB-185 778)
- WBTM TDL 25 Charts Giving Station Precipitation in the Plateau States From 850- and 500-Millibar Lows During Winter. August F. Korte, Donald L. Jorgensen, and William H. Klein, September 1969. (PB-187 476)
- WBTM TDL 26 Computer Forecasts of Maximum and Minimum Surface Temperatures. William H. Klein, Frank Lewis, and George P. Casely, October 1969. (PB-189 105)
- WBTM TDL 27 An Operational Method for Objectively Forecasting Probability of Precipitation. Harry R. Glahn and Dale A. Lowry, October 1969. (PB-188 660)
- WBTM TDL 28 Techniques for Forecasting Low Water Occurrences at Baltimore and Norfolk. Lt. (jg) James M. McClelland, USESSA, March 1970. (PB-191 744)
- WBTM TDL 29 A Method for Predicting Surface Winds. Harry R. Glahn, March 1970. (PB-191 745)
- WBTM TDL 30 Summary of Selected Reference Material on the Oceanographic Phenomena of Tides, Storm Surges, Waves, and Breakers. Arthur N. Pore, May 1970. (PB-193 449)
- WBTM TDL 31 Persistence of Precipitation at 108 Cities in the Conterminous United States. Donald L. Jorgensen and William H. Klein, May 1970. (PB-193 599)
- WBTM TDL 32 Computer-Produced Worded Forecasts. Harry R. Glahn, June 1970. (PB-194 262)
- WBTM TDL 33 Calculation of Precipitable Water. L. P. Harrison, June 1970. (PB-193 600)
- WBTM TDL 34 An Objective Method for Forecasting Winds Over Lake Erie and Lake Ontario. Celso S. Barrientos, August 1970. (PB-194 586)
- WBTM TDL 35 A Probabilistic Prediction in Meteorology: A Bibliography. A. H. Murphy and R. A. Allen, June 1970. (PB-194 415)
- WBTM TDL 36 Current High Altitude Observations--Investigation and Possible Improvement. M. A. Alaka and R. C. Elvander, July 1970. (Com-71-00003)

NOAA Technical Memorandum

- NWS TDL 37 Prediction of Surface Dew Point Temperatures. R. C. Elvander, January 1971. (Com-71-00253)
- NWS TDL 38 Objectively Computed Surface Diagnostic Fields. Robert J. Bermowitz, February 1971. (Com-71-00301)
- NWS TDL 39 Computer Prediction of Precipitation Probability for 108 Cities in the United States. William H. Klein, February 1971. (Com-71-00249)
- NWS TDL 40 Wave Climatology for the Great Lakes. N. A. Pore, J. M. McClelland, and C. S. Barrientos, February 1971. (Com-71-00368)
- NWS TDL 41 Twice-Daily Mean Monthly Heights in the Troposphere Over North America and Vicinity. August F. Korte, June 1971. (Com-71-00826)
- NWS TDL 42 Some Experiments With A Fine-Mesh 500-Millibar Barotropic Model. Robert J. Bermowitz, August 1971.

1

1